Published in Terra Nova 16 : 232-242, 2004,
which should be used for any reference to this work

Brittle deformation in the inner NW Alps: from early orogen-parallel extrusion to late orogen-perpendicular collapse

Jean-Daniel Champagnac, Christian Sue, Bastien Delacou and Martin Burkhard
Neuchatel University, Switzerland

ABSTRACT

Internal parts of the Alps have undergone widespread extensional deformation in the course of their Neogene exhumation history. Palaeostress inversion methods are used to map the prevailing stress fields and their evolution through time. Here we present new data from 100 sites with a total of about 2000 faults/striae couples, covering a large portion of the inner north-western Alps. Palaeostress tensors are mostly extensional, although one-third of them are transcurrent. The dominant direction of minimum horizontal stress axes (σ3) is in an orogen-parallel (N30° to N70°) orientation around the bend of the north-west alpine arc. A comparison between this older (Neogene, post-metamorphic) stress field with the current stress and strain field determined from seismotectonics and geodesy indicates a change in deformation mode from early orogen-parallel extrusion to a late and ongoing orogen-perpendicular spreading.

Introduction

The alpine orogen is the result of the Apulian/European convergence from the upper Cretaceous to Miocene (e.g. Steck, 1984; Escher *et al*., 1997; Pfiffner *et al*., 2000). On the continental scale, Africa currently converges with Europe at a rate from 3 to 8 mm yr^{-1} at the longitude of the western Alps (Demets *et al*., 1994; Albarello *et al*., 1995; Nocquet and Calais, 2003, 2004). On the alpine scale, however, geodetic measurements in the last decade have failed to demonstrate any convergence or other significant relative movement between northern Italy and 'stable Europe' (Calais *et al*., 2002; Oldow *et al*., 2002; Vigny *et al*., 2002). It now appears that Africa–Europe convergence is mostly consumed in a complex mobile zone which involves the Appenines, Dinarides and Magrebides.

Seismotectonic studies from the western Alps have revealed a predominance of transcurrent to extensional focal plane mechanisms; compressive focal plane mechanisms are rare and exclusively localized near the periphery of the alpine chain (Eva and Solarino, 1998; Sue *et al*., 1999; Delacou *et al*., in press a).

Correspondence: Jean-Daniel Champagnac, Institut de Géologie, Rue Emile Argand 11, CH-2007 Neuchâtel, Switzerland. Tel.: +41 32 718 26 57; fax: +41 32 718 26 01; e-mail: jean-daniel.champagnac@unine.ch

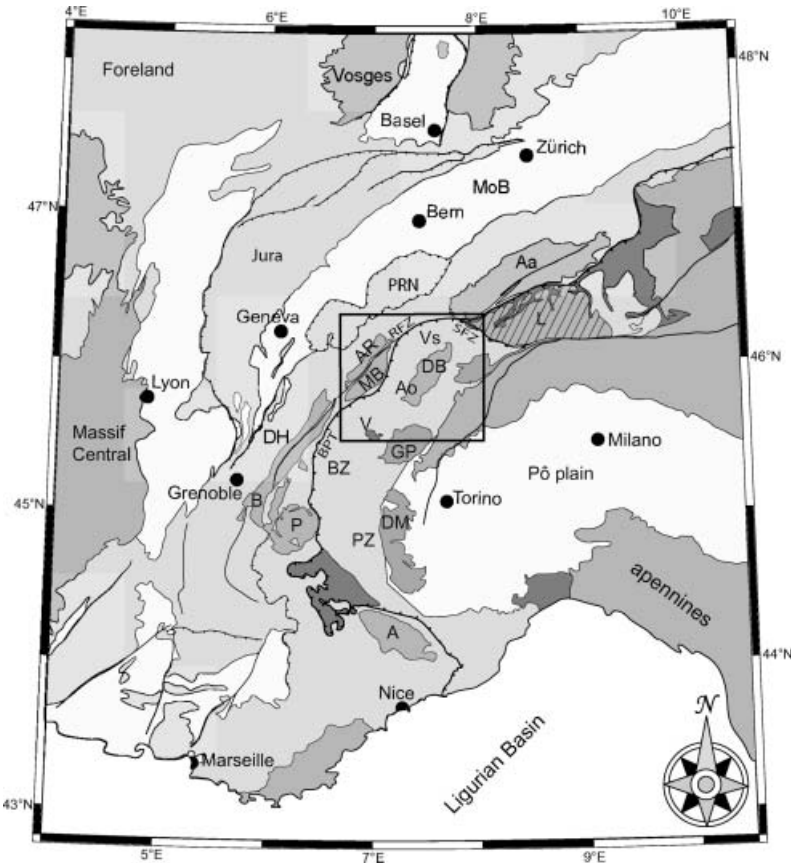

Fig. 1 Location of the studied area in the western Alps. A: Argentera; Aa: Aar; Ao: Aosta Valley; AR: Aiguilles Rouges; B: Belledonne; BPT: Basal Penninic Thrust; BZ: Briançonnais zone; DB: Dent Blanche nappe; DH: Dauphiné/Helvetic zone; DM: Dora Maira; GP: Gran Paradiso; L: Lepontine dome; MoB: Molasse Bassin; MB: Mont Blanc; PZ: Piémontais zone; P: Pelvoux; PRN: Prealpine Nappes; RFZ: Rhône Fault Zone; SFZ: Simplon Fault Zone; V: Vanoise; Vs: Valais.

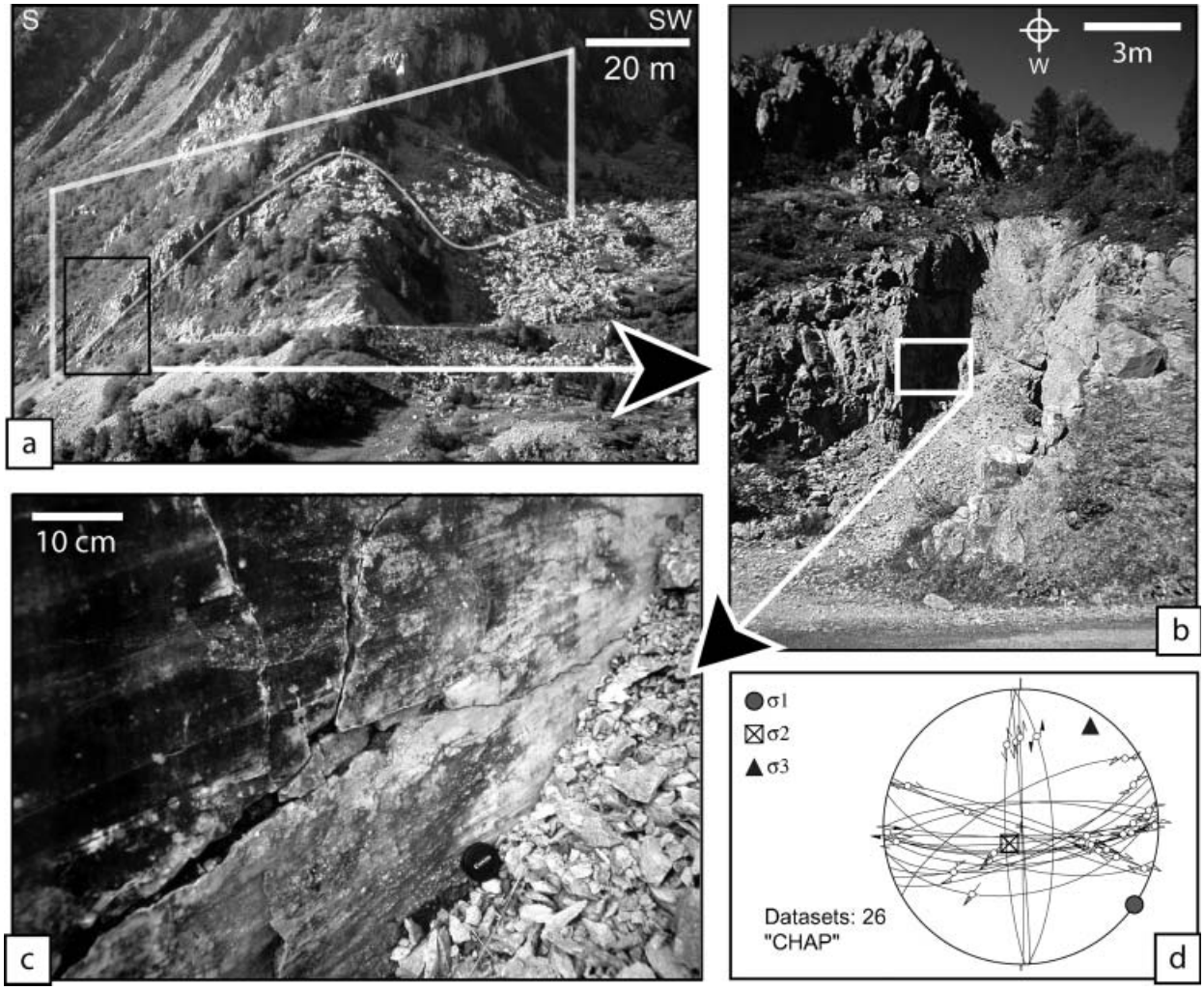

Fig. 2 (a) Morphological expression of a kilometric length fault (the 'Chapieux–Roseland' Fault viewed from the north). The movement along the nearly vertical fault plane is transcurrent. (b) Outcrop-scale view of the same fault. The fault plane is vertical, and associated with a thick fault gouge (about 4 m). This tectonic clay is the expression of a large amount of displacement, under conditions of low temperature and low fluid pressure, probably close to the surface. (c) Small-scale observation of the same fault shows a very slick fault plane, with horizontal and curved mechanical scratches. The fault plane cross-cuts an older cataclasite, with millimetric to centimetric broken then consolidated elements. There is no mineralization on the plane. (d) Measurements of several fault planes in this sector allow us to calculate the local palaeostress tensor. The major fault belongs to an east–west fault family, conjugated with a north–south more discrete fault family. The calculated tensor indicates a transcurrent stress field, with a N35° orientated σ3 and N125° orientated σ1.

Alpine extensional tectonics has been shown to have begun at an early stage, during the Late Oligocene – Early Miocene, at a time when thrusting was still active in external fold-and-thrust belts (e.g. Hubbard and Mancktelow, 1992; Steck and Hunziker, 1994; Tricart *et al*., 2001). Latest extensional structures under brittle conditions have been locally studied in the western Alps (Sue and Tricart, 1999, 2002, 2003; Bistacchi and Massironi, 2000; Agard *et al*., 2003; Champagnac *et al*., 2003; Grosjean *et al*., in press). This brittle deformation post-dates folds, schistosities and nappe-related structures. We focus here on the brittle deformation of the inner north-western Alps, between the Lepontine dome to the north-east, the Mont Blanc massif to the west and the Vanoise massif to the south (Fig. 1).

Our analysis is based on the determination of palaeostresses from a large faults/striae database. The palaeostress field constrains the post-nappe deformation of the studied area, which allows us to understand better the Neogene kinematics of the belt.

Geological and tectonic setting

The studied area is located in the southern Valais, the Aosta and the Tarentaise valleys (Fig. 1). This area belongs to the internal zones of the western Alps and is made up of upper penninic nappes (Briançonnais zone) overridden by the Piémontais suture zone and the Dent–Blanche nappe. The metamorphic history of the penninic units is complex and ranges from high to ultrahigh pressure for the Piémontais suture to moderate pressure (middle to upper greenschist facies) for most of

Table 1 Parameters and name of the 117 palaeostress tensors with the location (longitude and latitude in decimal degrees and altitude in metres), the σ1, σ2 and σ3 orientation (azimuth and plunge) and ellipsoid form parameter Φ. Also given are the number of faults used for the computation (*N*), the average misfit angle (α in degrees) and the quality criterion for the tensor (Conf.)

No.	Site	Lon.	Lat.	Alt.	σ1	σ2	σ3	Φ	*N*	α	Conf.
1	anniv (1)	7.5641	46.2645	1000	271/71	082/17	174/09	0.52	12	6	1
2	anniv (2)	7.5641	46.2645	1000	283/37	068/47	178/18	0.49	10	5.7	3
3	artsin	7.4279	46.1166	2960	008/61	207/27	113/08	0.47	18	11.5	1
4	cargn	7.5589	46.2326	1400	285/73	118/17	027/04	0.08	18	6.5	2
5	chevre	7.4318	46.0181	2870	214/69	038/21	307/01	0.2	11	5.5	2
6	cleus1	7.3219	46.1148	2100	315/69	172/17	079/12	0.06	12	2.9	2
7	cleus2	7.327	46.1094	2200	355/53	148/33	247/13	0.32	11	3.2	1
8	couta	7.4913	46.0824	1910	026/87	154/02	244/02	0.22	22	9.4	1
9	danger	7.3227	46.0212	1700	320/48	101/35	206/20	0.95	16	6.7	1
10	dix	7.4073	46.0887	2000	182/09	069/67	271/21	0.97	33	7.3	2
11	emdd (1)	7.8388	46.223	1380	210/71	309/03	040/19	0.06	22	4.8	2
12	emdd (2)	7.8388	46.223	1380	250/12	088/78	341/03	0.24	13	7.8	3
13	emmd2	7.8609	46.2319	1080	202/81	303/02	033/08	0.07	16	7.6	1
14	ergi1	7.7082	46.2959	1080	250/74	134/07	042/14	0.4	11	5.3	2
15	ergi2	7.7062	46.2898	828	226/64	002/19	098/17	0.93	9	9.8	3
16	evole	7.5043	46.1085	1500	002/53	131/25	233/25	0.26	28	4.3	1
17	findel	7.7856	46.0126	2200	179/36	326/49	076/17	0.77	21	9.7	2
18	forcl	7.4563	46.0302	2800	020/64	164/21	260/14	0.45	15	7.7	1
19	furi (1)	7.7326	45.9992	1860	178/63	026/25	291/11	0.08	21	6.3	1
20	furi (2)	7.7326	45.9992	1860	005/01	107/83	275/07	0.91	9	5	2
21	gallen	7.7891	46.0486	2300	053/59	309/08	215/30	0.79	9	4.3	2
22	gorner	7.7867	45.9847	3195	130/75	227/02	315/15	0.04	16	10	2
23	grime	7.5604	46.1609	1921	129/82	340/07	249/04	0.32	29	8.6	1
24	ires	7.2418	46.0733	1400	261/49	048/36	151/17	0.24	9	7.6	3
25	leuker	7.6603	46.3134	900	129/58	344/27	146/16	0.23	18	7	2
26	moiry (1)	7.5769	46.1122	2324	002/32	124/40	248/34	0.45	28	10.3	1
27	moiry (2)	7.5769	46.1122	2324	277/03	151/84	008/04	0.63	24	16.5	3
28	monv1	7.3596	45.9852	2100	048/69	204/19	296/08	0.11	13	6.3	3
29	monv2	7.3415	46.005	1820	334/13	196/72	064/11	0.49	25	9.6	1
30	nax	7.4597	46.2412	1020	318/82	151/08	061/02	0.22	9	6.1	3
31	nikla	7.7879	46.1638	1500	152/05	034/79	243/10	0.49	22	12.5	2
32	randa1	7.7751	46.0878	1600	105/59	241/24	340/19	0.78	13	13.6	3
33	randa2	7.7615	46.0847	2090	107/73	287/17	017/00	0.13	27	7.5	1
34	rech1 (1)	7.4992	46.2461	1010	022/23	326/62	118/14	0.78	9	2	2
35	rech1 (2)	7.4992	46.2461	1010	209/68	058/19	325/10	0.13	13	5	2
36	rech2	7.4953	46.2416	1200	173/76	276/03	007/14	0.03	19	8.9	1
37	rotba	7.8215	46.0656	2550	350/46	138/39	242/16	0.04	14	2.4	2
38	roten	7.7674	45.9866	2820	258/08	019/75	167/12	0.75	12	5.5	2
39	sarray	7.2593	46.0606	1129	353/51	148/37	247/12	0.87	16	4.8	1
40	schler	7.2715	46.0697	2000	239/65	137/05	045/24	0.16	8	3.8	3
41	solay1	7.5481	46.0653	1800	329/22	195/60	067/19	0.06	8	6.2	3
42	solay2	7.5385	46.0743	1700	150/71	349/18	257/06	0.17	16	8.6	2
43	solay3	7.534	46.0761	1700	000/50	212/36	110/16	0.98	11	3.5	3
44	stlu1	7.5939	46.2312	1720	178/67	331/21	065/10	0.23	13	3.3	1
45	stlu2	7.6029	46.2182	1580	151/37	353/51	249/11	0.6	15	6.3	2
46	tdela	7.3743	46.1571	2160	238/61	091/25	354/14	0.08	16	3.9	3
47	thyon	7.3709	46.1787	2160	262/70	142/10	049/17	0.29	14	6.3	2
48	trift	7.4505	46.0245	1800	123/81	288/09	018/02	0.33	35	8.7	1
49	turgl	7.7096	46.1496	2728	049/89	175/01	265/01	0.83	15	10.4	2
50	turtm	7.6913	46.1714	2150	022/57	147/21	247/25	0.24	27	7.5	1
51	verc1	7.4558	46.2582	1151	147/73	287/13	020/11	0.01	19	11.4	2
52	verc2	7.5433	46.2479	1350	122/73	325/16	233/06	0.3	18	10.6	2
53	veyso	7.3321	46.194	1000	118/65	323/23	229/09	0.14	9	3.8	2
54	vingt	7.3956	46.0752	2380	271/81	173/01	083/09	0.57	16	3.8	1
55	visso	7.5809	46.2344	1100	205/08	091/71	298/17	0.85	17	5.6	3
56	zeneg	7.871	46.2795	1350	300/19	082/67	206/13	0.59	20	6.2	3
57	AVISE	7.1526	45.7059	775	005/63	128/16	224/22	0.05	17	7.3	1
58	BAUCHE	6.7464	45.5394	1702	009/75	177/15	268/03	0.62	18	5.9	1
59	BISELX	7.2227	46.0058	2520	218/58	107/13	107/13	0.99	16	2.8	2
60	BUTHIER	7.2713	45.7845	1277	273/49	111/40	013/09	0.32	16	5.1	1

Table 1 Continued

No.	Site	Lon.	Lat.	Alt.	σ1	σ2	σ3	Φ	*N*	α	Conf.
61	CARLO	7.003	45.7136	2000	050/65	150/05	242/24	0.9	20	8.1	1
62	CHAP	6.7318	45.6937	1600	343/08	249/30	087/59	0.36	16	10.1	2
63	CHAT1	6.858	45.6178	1470	183/72	079/05	348/17	0.26	15	7.8	3
64	CHAT2	6.8628	45.4148	1378	218/61	119/05	027/28	0.01	18	1.8	1
65	ECHEV	7.2638	45.8026	1200	031/61	205/29	296/02	0.52	28	4	1
66	FRETE (1)	6.8085	45.5709	2384	268/55	051/29	151/17	0.07	17	4	1
67	FRETE (2)	6.8085	45.5709	2384	291/08	147/80	022/06	0.57	8	10.2	3
68	GSB1	7.1877	45.8865	2120	101/11	215/65	007/22	0.91	21	7.7	3
69	GSB2	7.1896	45.8995	1980	313/24	159/64	047/10	0.58	19	16.9	2
70	GSBIT	7.1512	45.8598	2120	347/25	108/48	241/32	0.37	15	4.6	2
71	GURRAZ	6.9033	45.6249	1400	359/75	142/12	234/09	0.23	24	6.1	1
72	ISERAN	7.021	45.4317	2620	084/84	352/00	262/06	0.20	34	9.4	1
73	LACPLAG	6.845	45.488	2224	319/65	141/25	051/01	0.07	14	3.7	2
74	MALAT	7.1313	45.8409	2060	271/32	129/52	013/19	0.18	15	4.7	2
75	MALAT2	7.1113	45.8408	2200	275/21	117/67	008/08	0.25	14	4.3	2
76	MARTI	7.0814	46.0918	860	325/22	231/10	118/65	0.58	11	9.7	3
77	MICOEUR	7.2449	46.1183	2240	136/73	302/16	033/04	0.55	10	6.8	3
78	MONAL (1)	6.9009	45.5687	1800	048/85	165/02	255/04	0.25	20	11.8	1
79	MONAL (2)	6.9009	45.5687	1800	119/36	298/54	029/00	0.54	11	6.2	2
80	NIORD	7.2035	45.9589	1560	261/02	168/59	352/31	0.57	16	9.2	2
81	PEIPOU	6.818	45.5253	2000	142/76	142/76	241/02	0.25	22	13	1
82	PLAN	6.9258	45.6244	1940	284/16	039/55	185/30	0.60	14	9	2
83	RECUL	6.9618	45.4669	1810	171/69	031/17	297/13	0.16	19	10.1	1
84	RIDD	7.2233	46.1551	1030	119/68	264/19	358/12	0.81	22	8.8	2
85	SAPIN	7.1486	46.1063	1600	352/73	151/16	243/06	0.77	15	7.8	2
86	SEIGNE	6.8091	45.7528	2500	308/48	082/32	188/24	0.78	17	7.1	2
87	STFOY (1)	6.9313	45.5787	2680	091/56	359/02	267/34	0.70	16	4	1
88	STFOY (2)	6.9313	45.5787	2680	157/11	048/61	253/27	0.49	14	7.1	2
89	THUIL	6.8991	45.7203	1920	088/71	265/19	355/01	0.53	10	4	3
90	TIGNES1	6.9199	45.5054	1620	032/73	129/02	220/17	0.13	17	5.1	1
91	TIGNES2	6.9254	45.4539	1850	195/25	060/56	295/21	0.42	13	7.3	2
92	TIGNES3	6.9442	45.4977	1800	065/75	280/12	188/08	0.81	11	4.3	2
93	TOULJE	7.1882	45.922	2000	300/47	145/40	044/13	0.87	24	6.5	2
94	VALDER1	7.1055	45.54	1880	316/51	209/13	110/36	0.07	12	3.6	2
95	VALDER2	7.1119	45.546	1800	272/78	115/11	024/05	0.33	13	6.6	1
96	VALDER3	7.122	45.5882	1800	083/50	248/39	344/07	0.92	11	6.5	3
97	VALDER4 (1)	7.0259	45.6242	1540	079/79	303/08	212/08	0.05	10	14.7	2
98	VALDER4 (2)	7.0259	45.6242	1540	247/03	343/63	155/26	0.65	12	2.9	2
99	VALGR1	7.1562	45.6978	800	036/73	271/10	178/14	0.09	12	4.1	2
100	VALGR25	7.0482	45.6041	1800	016/56	183/33	277/06	0.74	22	10.5	2
101	VALGR3	7.0632	45.6206	1800	228/87	126/01	036/03	0.50	12	5.1	2
102	VALGR4	7.1008	45.679	1420	319/39	204/28	089/38	0.95	20	4.5	2
103	VALP1 (1)	7.2974	45.8715	1635	026/05	168/84	296/04	0.76	17	8.8	2
104	VALP1 (2)	7.2974	45.8715	1635	117/78	009/04	279/11	0.62	21	9.6	3
105	VALP2 (1)	7.4924	45.9007	1800	161/57	312/30	049/13	0.35	12	11.4	2
106	VALP2 (2)	7.4924	45.9007	1800	098/31	188/59	190/04	0.95	11	5.1	3
107	VALP3	7.4628	45.8881	1730	196/85	099/01	009/05	0.71	13	6.1	2
108	VALP4 (1)	7.437	45.8782	1710	094/04	294/86	184/01	0.26	14	6.8	3
109	VALP4 (2)	7.437	45.8782	1710	359/75	155/13	246/06	0.07	17	8	1
110	VALP5	7.3534	45.8323	1600	301/38	122/55	031/00	0.55	17	7	3
111	VALSA1 (1)	7.2008	45.5295	2040	088/45	319/32	210/27	0.13	11	3	2
112	VALSA1 (2)	7.2008	45.5295	2040	101/35	322/47	207/21	0.51	10	8.6	3
113	VALSA2	7.2115	45.5228	1800	091/36	327/38	208/32	0.48	11	4.1	3
114	VALSA3	7.2032	45.6525	1180	028/79	139/04	229/11	0.16	10	4.2	2
115	VALSA4	7.2051	45.6742	1140	093/70	304/17	211/10	0.77	16	14.4	2
116	VELAN	7.2591	45.9267	2410	300/01	201/85	030/05	0.50	16	8	2
117	VENS	7.1241	46.0865	1100	278/08	165/70	011/19	0.63	26	19.9	3

the basement (see Frey *et al*., 1999, for further details). Several major fault zones border the study area:

To the north-east, the Simplon fault zone has been described as a major NW–SE detachment with a long history including ductile and brittle extension since the Early Miocene (Mancktelow, 1985, 1992; Mancel

and Merle, 1987; Grosjean *et al*., in press).

To the north, the Rhône Fault Zone (RFZ) follows the Basal Penninic Thrust (BPT) beneath the Rhône valley. Normal and dextral movements have been determined along the RFZ (Burkhard, 1990; Hubbard and Mancktelow, 1992; Steck and Hunziker, 1994). Based on apatite fission tracks, a Late Miocene age of normal faulting has been postulated for this fault (Soom, 1990; Seward and Mancktelow, 1994). Morphological features, such as inverse slopes immediately south of the Rhône valley, also suggest a very recent age of normal faulting (Champagnac *et al*., 2003). Seismic activity in the north Valais area shows a dextral transcurrent mode, but north–south extension in the southern Valais (Maurer *et al*., 1997; Delacou *et al*., in press a). The RFZ cuts westward within the Chamonix syncline as a transpressive dextral zone between the Mont-Blanc and Aiguilles-Rouges External Crystalline Massifs (ECM) (Gourlay and Ricou, 1983).

To the west, the BPT borders the internal side of the Mont-Blanc massif, orientated NNE–SSW. The BPT separates the Helvetic units (ECM and their Mesozoic cover) and the overridden Penninic units. This contact is a thrust of Late Oligocene – Early Miocene age (Steck and Hunziker, 1994). A subsequent normal reactivation of the BPT has been locally observed and could be interpreted as due to Miocene exhumation of the ECM (Seward and Mancktelow, 1994; Aillères *et al*., 1995; Cannic *et al*., 1999; Sue and Tricart, 1999).

In the core of our study area, the Aosta valley is the morphological expression of the major Aosta–Ranzola fault zone. It has been described as a north-dipping Oligocene normal fault, reactivated as a sinistral transcurrent fault zone from the Miocene to the Present (Carraro *et al*., 1994; Bistacchi *et al*., 2001).

Data analysis

We used field observations at different scales (example on Fig. 2), and a systematic collection of minor faults (in the 0.1–1 m range) to determine palaeostress axis directions using the 'direct inversion method' of Angelier (1990) implemented in the 'tectonics FP' software (Sperner *et al*., 1993). About 2000 fault planes and their slickensides were measured at 100 sites. Locally, two superimposed brittle deformation stages have been observed; their relative chronology has been deduced from cross-cutting relationships between fault planes and/or slickensides. At several sites, systematically curved slickensides indicate a progressive change of fault movement.

The stability and the quality of each tensor were estimated from a series of criteria, including a first coherency test using the right-dihedra method of Angelier and Mechler (1977), visualization of the inverse function (Yamaji, 2000), the number of faults used in the inversion and the average misfit angle. Tensors were classified from 1 (excellent) to 3 (low quality). We calculate in this way 117 palaeostress tensors (Fig. 3a and Table 1).

Most of these stress tensors are extensional (steep σ1, subhorizontal σ2 and σ3). The predominant direction of extension (σ3) is NE–SW. About 30% of our palaeostress tensors are transcurrent (steep σ2, subhorizontal σ1 and σ3).

The direction of the σ3 axes is almost the same for transcurrent and extensional tensors; furthermore, the relative chronologies change within small or larger areas, with frequently curved slickensides. We regard the extensional and transcurent stress field

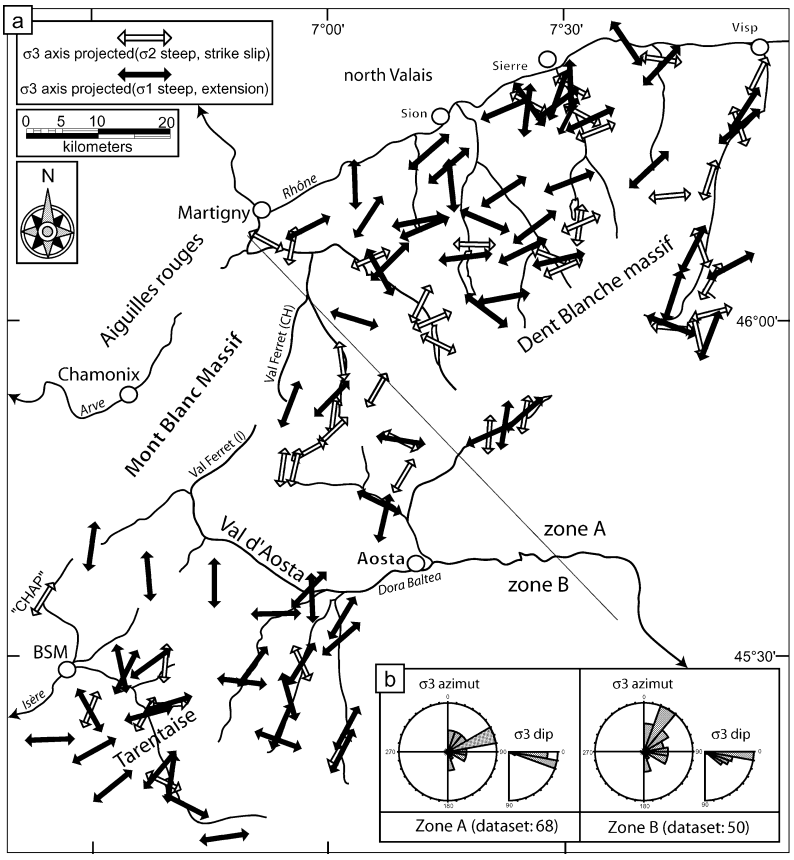

Fig. 3 (a) Palaeostress map, with σ3 subhorizontal axes projected; white arrow for strike-slip tensors (subhorizontal σ1), black arrows for extensional tensors (subvertical σ1). The trend of the σ3 axes appears globally NE–SW. 'BSM', Bourg-Saint-Maurice. (b) The 20° class-size rose-diagram in the inset represents the σ3 axes orientations and dips for zones A (the Valais area) and B (the Gran San Bernardo, Aosta and Tarentaise Valleys). The most frequent direction is about N70° in zone A and N30° in zone B, i.e. in an orogen-parallel direction. Note that the σ3 axes dip always gently, at less than 20°.

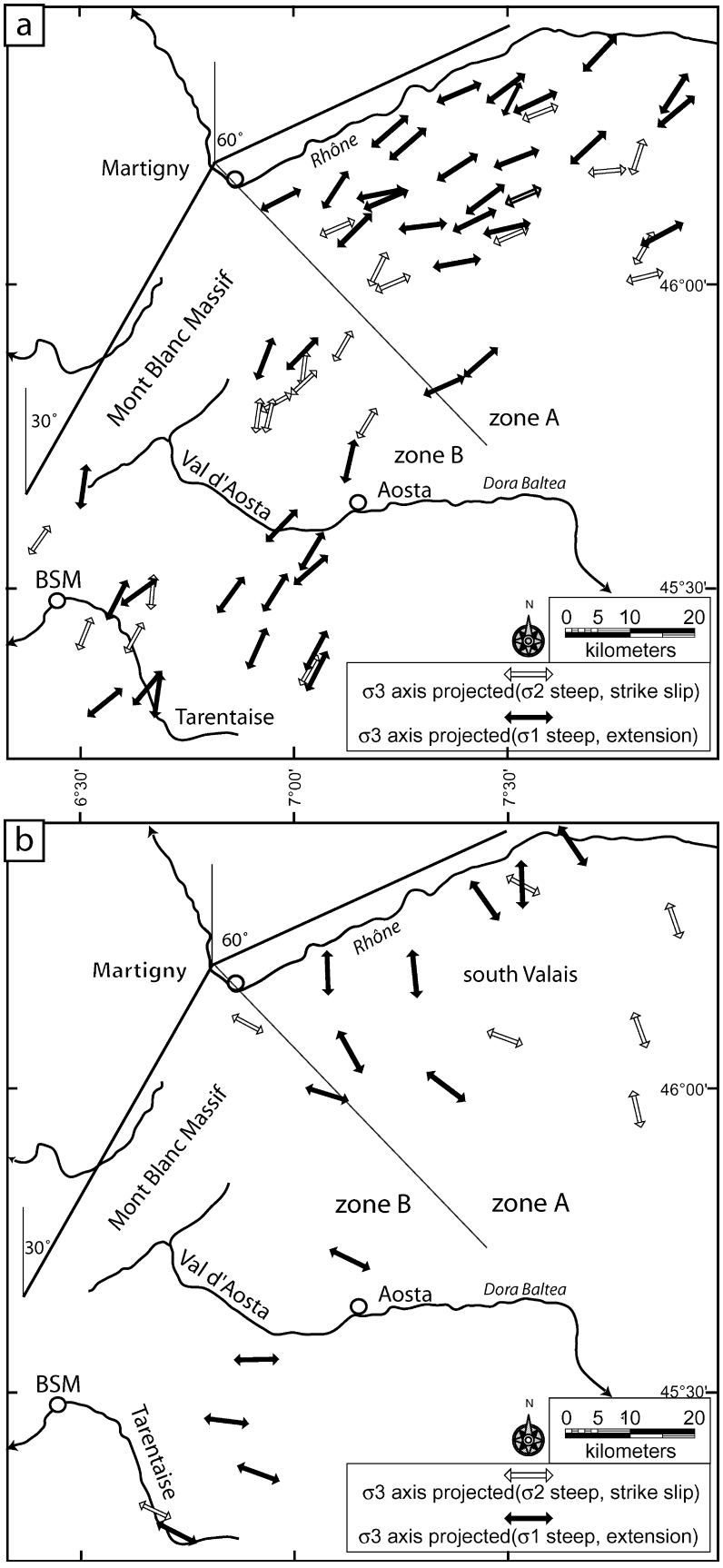

Fig. 4 (a) Representation of the orogen-parallel direction of minimum stress axes ($\beta < 30°$, where β is the angle between the alpine trend and the $\sigma 3$ orientation). These represent more than 50% of the database. The $\sigma 3$ orientations describe a wide arc in the studied area, from the Simplon pass to the Tarentaise Valley. The ratio of transcurrent tensors is about 30%. (b) Representation of the orogen-perpendicular direction of minimum stress axes ($\beta > 60°$). The axes describe a large fan, which could be linked to the active stress field.

as a single 'stage', with a local or temporal relative swapping of the $\sigma 1$ and $\sigma 2$ axes.

Based on this assumption, we consider only the $\sigma 3$ axis orientation for the following discussion, regardless of the $\sigma 1$ axis being subvertical or subhorizontal. The general direction of the $\sigma 3$ palaeostress axes throughout the study area is orientated in a NE–SW direction, mimicking the trend of the alpine belt. In order to quantify this angular relationship between the palaeostress tensor orientations and the alpine structural trend we separated the north-west Alpine arc in two parts (Fig. 3a): a NE area (A), which corresponds to an 'Aar-like' orientation (strike N60°) from Visp to Martigny; and a second SW area (B), which corresponds to a 'Mont Blanc-like' orientation (strike N30°) from Martigny to Bourg-Saint-Maurice. The line between zone A and B strikes N120°. Average $\sigma 3$ orientations demonstrate a generalized orogen-parallel extension, N70° orientated in zone A, N30° orientated in zone B (Fig. 3b).

In this crude statistical analysis, 50% (68%) of our palaeostress tensors show less than 30° (45°, respectively) between their strike and the alpine trend (β) (Fig. 4a).

The $\sigma 3$ axes trajectories describe a wide arc in the whole Simplon–Vanoise area and provide a large-scale image of a brittle orogen-parallel extension event in the inner north-western Alps.

Significant deviations from this simple picture are observed in 19 out of 117 tensors, which indicate an 'orogen-perpendicular' direction at high angle ($\beta > 60°$) to the strike

of the belt. Together, these tensors describe a large-scale fan from the eastern Valais to the Vanoise area (Fig. 4b). Orogen-perpendicular extension is currently ongoing in central parts of the western Alps according to focal mechanisms (Sue and Tricart, 2003; Delacou *et al*., in press b). In the NW Alps, the passage from orogen-parallel to orogen-perpendicular extension may also be interpreted as stress axis permutation between σ2 and σ3, with low Φ ratio, as proposed by Sue and Tricart (2002) in the SW Alps. Actually we propose a two-stage interpretation because of the similarity with the seismologically active inferred stress field.

One-third of all the tensors are neither in an orogen-parallel nor in an orogen-perpendicular direction, with σ3 oblique with respect to the main alpine structure ($30° < \beta < 60°$). This is explained in terms of local deviations of the overall stress field, including tilted and rotated blocks of unknown dimension. The dispersion of the mean σ1 around the vertical axis (Fig. 5) can similarly be explained.

In order to analyse the palaeostress ellipsoid shape (the relative magnitude of σ1, σ2 and σ3), we used the Φ ratio [$\Phi = (\sigma1 - \sigma3)/(\sigma2 - \sigma3)$]. Using this approach, we analysed our database in terms of Φ ratio, plotting Φ vs. the dip of the σ1 axis for each tensor (Fig. 5) in a polar graph. We separate this diagram into five parts (see figure caption for details). Forty per cent of the tensors are 'multitrend-extensional', with a good average quality criterion. Twenty-five and 20% of transtensive and transcurrent tensors, respectively, are generally of medium quality.

In summary, the inversion of brittle deformation structures (faults and striae) documents a large-scale palaeostress field, which is mainly extensional. This extension is mixed with transcurrent and transtensive palaeostress tensors that exhibit the same strike-parallel direction of the minimal stress axis (σ3). The orogen-parallel direction of σ3 is the major first-order signal for the Neogene stress field. A more discrete orogen-perpendicular direction of extension, probably younger, is also observed.

Discussion and conclusion

Extension in the core of mountain belts is a common feature that has been observed worldwide (Wernicke and Burchfield, 1982; Dewey, 1988; Rey *et al*., 2001). Coaxial extension, opposite to the direction of the converging plates, as observed in the Andes (Dalmayrac and Molnar, 1981; Deverchere, 1988), the Himalayas (Molnar and Tapponnier, 1978; Herren, 1987) and the Basin and Range (Lister and Davis, 1989), has mostly been interpreted in terms of orogenic collapse. Extension is due to the subtle interplay between the rates of convergence (decreasing), internal strain, external erosion and the temperature/time-dependent internal strength of the orogenic wedge (Avouac and Burov, 1996).

Synorogenic extension is well documented for many parts of the internal Alps, all along the crestline from the eastern Alps (Selverstone, 1988; Ratschbacher *et al*., 1991; Decker and Peresson, 1996; Linzer *et al*., 2002) through the central Alps (Mancktelow, 1990, 1992; Nievergelt *et al*., 1996) to the western Alps (see references above). In contrast to those orogens with coaxial collapse

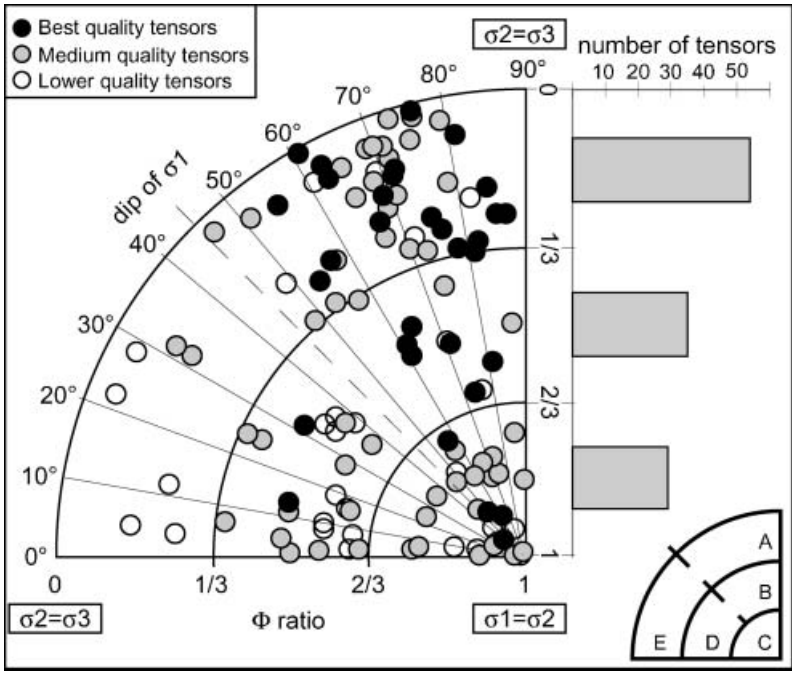

Fig. 5 Representation of the Φ ratio vs. the dip of σ1 in a polar representation (left part) and histogram of the Φ ratio (right part). In the case of extensional tensors (σ1 steep), a low Φ ratio implies similar σ2 and σ3, indicating multitrend extension; a high Φ ratio implies similar σ1 and σ2, indicating transtension; an intermediate Φ ratio indicates a pure extensional tensor. For strike-slip tensors (subhorizontal σ1 and σ3), a low Φ ratio indicates transpression; a medium Φ ratio implies pure strike-slip and a high Φ ratio implies transtension. Black, grey and white circles represent best, medium and lower quality tensors, respectively. We separate the polar diagram into five parts. In A (σ1 more than 45° and Φ ratio less than 1/3), 47 multitrend extensional tensors (40% of the dataset) are plotted. They show very good quality criterion (average = 1.27). The relative magnitudes of σ2 and σ3 are almost similar. In B (σ1 more than 45° and Φ ratio between 1/3 and 2/3), few (11) pure-extensional tensors are plotted. Nevertheless, they have a high average quality criterion (= 1.63) and a good spatial coherency. In C (Φ ratio more than 2/3), 29 transtensive tensors (25% of the dataset) are plotted; they have a medium average quality criterion (= 2.1) and there is a continuum in the dip of σ1 (tilted tensors). In D (σ1 less than 45° and Φ ratio between 1/3 and 2/3), 24 strike slip tensors are plotted (20% of the dataset). Their average quality criterion is medium (2.29). In E (σ1 less than 45° and Φ ratio less than 1/3), seven transpressive tensors are plotted, with a poor average quality criterion (2.71); they probably have no regional significance.

previously mentioned, the main alpine extension direction is orientated along the strike of the chain. Accordingly, most authors working on this area propose various models of synorogenic lateral extrusion. Lateral extrusion to the east prevails from the Lepontine Dome eastward to the Pannonian basins, in response to 'back arc' extension behind the Carpathian arc. From the Simplon area westward, strike-parallel extension is observed around the 90° bend of the western Alps. The opening of the Ligurian basin during the Early Middle Miocene (Vigliotti and Langenheim, 1995; Carminati *et al*., 1998; Speranza *et al*., 2002) could be the free boundary necessary for such a large-scale orogen-parallel extension in the north-western Alps. The known strike slip faults are predominantly dextral, accommodating a relative south- and south-westward movement of internal parts of the Alps with respect to the radially 'forelandward thrust' external parts of the Alps (Hubbard and Mancktelow, 1992). Conjugate sinistral strike slip faults are not observed within the Alps proper and a direct comparison with the 'extruding' wedges (in map view) of the eastern Alps is not straightforward. The predominance of dextral strike slips and their radially changing orientation in a fan-like pattern has led some authors to consider rotation, rather than sideways extrusion as an alternative large-scale process at the NW tip of the Adriatic indenter (Goguel, 1963; Pavoni, 1991; Pavoni *et al*., 1997). Rotation models are supported by geomagnetic data that document large anticlockwise vertical axis rotations of up to 90° and more, increasing southward along the arc of the western Alps (Collombet *et al*., 2002). The extrusion tectonism we observed, particularly in the Simplon area, could be associated with the anticlockwise rotation shown by Hubbard and Mancktelow (1992) and Collombet *et al*. (2002). Our own fault measurements provide new evidence for a widespread arc-parallel extension all along the crest-line of the western Alps (Fig. 6). Given the brittle nature of faults used to establish palaeostress directions, this extension is clearly post-metamorphic. Its onset goes back to nearly peak temperature conditions. Furthermore, the wide variety of fault plane appearance (calcite, quartz, hematite or chlorite mineralization, cataclasite, fault breccia and gouges) suggests a long brittle history.

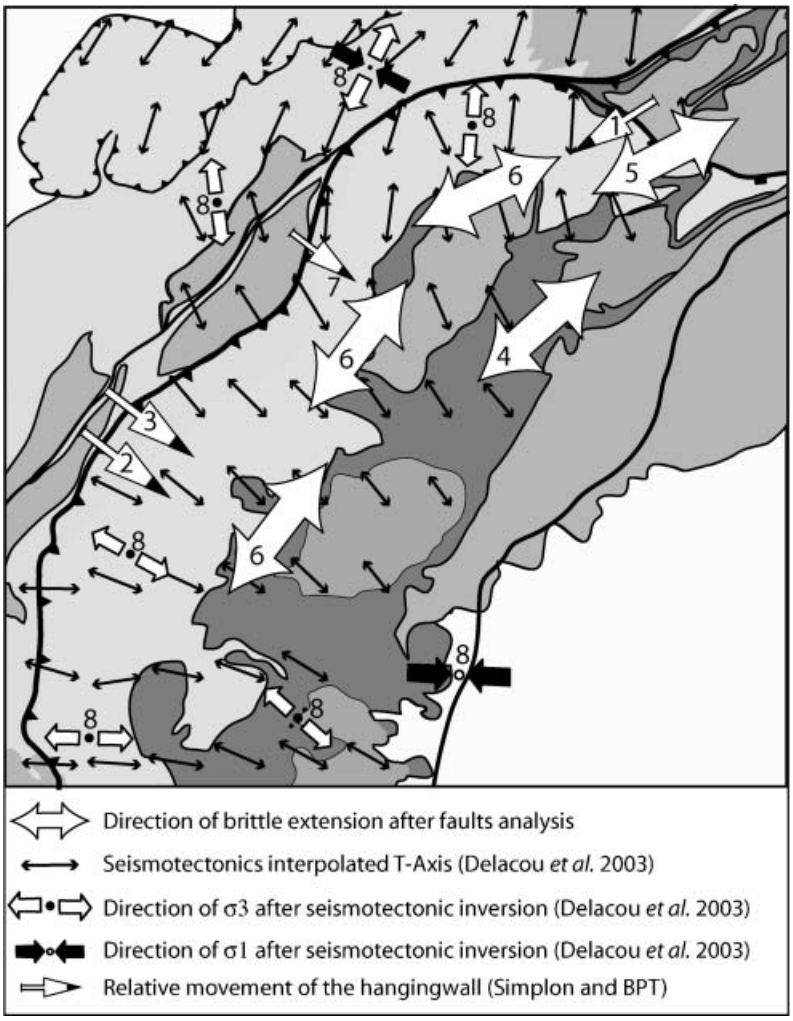

Fig. 6 Synthesis of the Neogene and still-active tectonics in the inner north-western Alps. (1) Ductile kinematics in the Simplon area (Mancktelow, 1992). (2) and (3) Ductile kinematics along the ECORS transect (Aillères *et al*., 1995; Cannic *et al*., 1999). (4) Brittle kinematics in the east of the Val d'Aosta (Bistacchi and Massironi, 2000). (5) Brittle kinematics in the Simplon pass area (Grosjean *et al*., in press). (6) Brittle kinematics of this paper and Champagnac *et al*. (2003). (7) Fission track analysis after Seward and Mancktelow (1994). (8) Current stress field based on seismotectonic inversion, after Delacou *et al*. (in press a,b).

Normal faulting, possibly with a component of dextral shearing along the Rhône line immediately to the west of the Simplon fault, is documented to be active up to the latest Miocene. Apatite fission track ages indicate a relative downthrow of the internal 'Penninic' units with respect to external 'Helvetic' nappes and crystalline massifs. Faulting is at least as young as 3 Ma, because palaeo-isotherms of this age are offset on either side of the Rhône valley (Soom, 1990; Seward and Mancktelow, 1994). The present state of stress within the Alps is now well documented following analysis of focal plane mechanisms all along the arc of the western Alps (Maurer *et al*., 1997; Sue *et al*., 1999; Kastrup *et al*., 2004; Delacou *et al*., in press b). Higher parts of the chain, near the crest-line of the Alps westward of the Lepontine Dome, are clearly in an extensional

state of stress at present. In contrast to the majority of palaeostress measurements, however, the current direction of extension is orogen-perpendicular. This orientation is reminiscent of the 'orogenic collapse' model and more difficult to reconcile with the idea of a lateral extrusion and/or rotation. It is tempting to interpret a minority of palaeostress measurements as belonging to this most recent deformation phase, although we do not have any direct evidence. A similar chronology (orogen-parrallel then orogen-perpendicular extension) has been observed in the eastern Alps (Decker *et al*., 1993).

Combined with seismotectonics, geodesy allows us to constrain present-day deformation rates within the Alps and between adjacent forelands (Kahle *et al*., 1997; Vigny *et al*., 2002). Up to 10 years of measurements now allow us to conclude that convergence between the NW tip of the Adriatic microplate and 'stable Europe' is not ongoing today (Calais *et al*., 2002; Oldow *et al*., 2002).

In summary, we conclude that two extension events of post-metamorphic faulting have affected central parts of the arc of the western Alps. From Late Oligocene throughout Miocene times, extension is orientated in an orogen-parallel direction, leading to a relative right-lateral movement to the south or south-west of internal parts of the Alps with respect to the north-west European foreland. This lateral extrusion event is no longer active. The current state of stress indicates fan-like extension directions at a high angle with respect to the strike of the Alpine arc. Collision must have come to a complete halt during the Plio-Pleistocene and the Western Alps are now in an early phase of post-orogenic collapse and decay.

Acknowledgements

This work was supported by the Neuchâtel University and by the Swiss National Science Found (grant no. 21-61684.00). We thank C. Allanic, M. Sartori and P. Tricart for fruitful discussions and comments. K. Decker and J.-P. Gratier provided constructive reviews and comments.

References

Agard, P., Fournier, M. and Lacombe, O., 2003. Post-nappe brittle extension in the inner Western Alps (Shistes Lustrés) following ductile exhumation: a record of synextension block rotation? *Terra Nova*, **15**, 000–000.

Aillères, L., Bertrand, J., Macaudière, J. and Champenois, M., 1995. New structural data from the "Zone Houillere Brianconnaise" (French Alps), neoalpine tectonics and consequences for the interpretation of the Pennine Front. *C.R. Acad. Sci. (Paris)*, **321**, 247–254.

Albarello, D., Mantovani, E., Babbucci, D. and Tamburelli, C., 1995. Africa-Eurasia kinematics – main constraints and uncertainties. *Tectonophysics*, **243**, 25–36.

Angelier, J., 1990. Inversion of field data in fault tectonics to obtain the regional stress – A new rapid direct inversion method by analytical means. *Geophys. J. Int*., **103**, 363–376.

Angelier, J. and Mechler, P., 1977. Sur une méthode graphique de recherche des contraintes principales également utilisable en tectonique et en sismologie: la méthode des dièdres droits. *Bull. Soc. Géol. France*, **7**, 1309–1318.

Avouac, J.P. and Burov, E.B., 1996. Erosion as a driving mechanism of intracontinental mountain growth. *J. Geophys. Res*., **101** (B8), 17747–17769.

Bistacchi, A., Dal Piaz, G.V., Massironi, M., Zattin, M. and Balestrieri, M.L., 2001. The Aosta–Ranzola extensional fault system and Oligocene– Present evolution of the Austroalpine-Penninic wedge in the northwestern Alps. *Int. J. Earth Sci*., **90**, 654–667.

Bistacchi, A. and Massironi, M., 2000. Post-nappe brittle tectonics and kinematic evolution of the north-western Alps: an integrated approach. *Tectonophysics*, **327**, 267–292.

Burkhard, M., 1990. Aspects of the large-scale Miocene deformation in the most external part of the Swiss Alps (Subalpine Molasse to Jura fold belt). *Eclog. Geol. Helv*., **83**, 559–583.

Calais, E., Nocquet, J.M., Jouanne, F. and Tardy, M., 2002. Current strain regime in the Western Alps from continuous Global Positioning System measurements, 1996–2001. *Geology*, **30**, 651–654.

Cannic, S., Mugnier, J.-L. and Lardeaux, J.-M., 1999. Neogene extension in the Western Alps. *Mem. Sci. Geol. Padova*, **51**, 33–45.

Carminati, E., Wortel, M.J.R., Spakman, W. and Sabadini, R., 1998. The role of slab detachment processes in the opening of the western-central Mediterranean basins: some geological and geophysical evidence. *Earth Planet. Sci. Lett*., **160**, 651–665.

Carraro, F., Guibaudo, G., Giardino, M. and Perotto, A., 1994. Intense deformazioni in depositi fluvioglacustri olocenici nella media valle d'Aosta. *Atti Tic. Sci. Terra*, **1**, 123–136.

Champagnac, J.D., Sue, C., Delacou, B. and Burkhard, M., 2003. Brittle orogen-parallel extension in the internal zones of the Swiss Alps (south Valais). *Eclog. Geol. Helv*., **96**, 325–338.

Collombet, M., Thomas, J.C., Chauvin, A., Tricart, P., Bouillin, J.P. and Gratier, J.P., 2002. Counterclockwise rotation of the western Alps since the Oligocene: new insights from paleomagnetic data. *Tectonics*, **21**, 352–366.

Dalmayrac, B. and Molnar, P., 1981. Parallel thrust and normal faulting in Peru and constraits on the state of stress. *Earth Planet. Sci. Lett*., **55**, 473–481.

Decker, K., Meschede, M. and Ring, U., 1993. Fault slip analysis along the northern margin of the Eastern Alps (Mollasse, Helvethic nappes, North- and South-Penninic flysch and the Northern Calcareous Alps). *Tectonophysics*, **223**, 291–312.

Decker, K. and Peresson, H., 1996. Tertiary kinematics in the Alpine-Carpathian-Pannonian system: links between thrusting, transform faulting and crustal extension. In: *Oil and Gas in Alpidic Trustbelts and Basins of Central and Eastern Europe* (G. Wessely and W. Liebl, eds), pp. 69–77. Spec. Publ. EAGE.

Delacou, B., Sue, C., Champagnac, J.D. and Burkhard, M., in press a. Origin of the current stress field in the western/central Alps: role of gravitational re-equilibration constrained by numerical modelling. *Geol. Soc. London DRT 2003 Spec. Publ*., in press.

Delacou, B., Sue, C., Champagnac, J.D. and Burkhard, M., in press b. Present-day geodynamics in the bend of the western and central Alps as constrained by earthquake analysis. *Geophys. J. Int*., in press.

Demets, C., Gordon, R.G., Argus, D.F. and Stein, S., 1994. Effect of recent revisions to the geomagnetic reversal time scale on estimates of current plate motions. *Geophys. Res. Lett*., **21**, 2191–2194.

Deverchere, J., 1988. *Extension crustale dans un contexte de convergence de plaques: l'exemple des Andes du Pérou central contraint par des données sismotectoniques*. PhD thesis, Orsay, Paris.

Dewey, J.F., 1988. Extensional collapse of orogens. *Tectonics*, **7**, 1123–1139.

Escher, A., Hunziker, J.C., Marthaler, M., Masson, H., Sartori, M. and Steck, A., 1997. Geological framework and structural evolution of the Western Swiss-Italian Alps. In: *Deep Structures of the Swiss Alps: Results of NRP20* (O.A. Pfiffner, P. Lehner, P. Heitzmann, S. Mueller and A. Steck, eds), pp. 205–222. Birkhaüser Verlag, Basel.

Eva, E. and Solarino, S., 1998. Variations of stress directions in the western Alpine arc. *Geophys. J. Int.*, **135**, 438–448.

Frey, N., Desmons, J. and Neubauer, F., 1999. Metamorphic maps of the Alps. *Schweiz. mineral. petrogr. Mitt.*, **79**, 1–4.

Goguel, J., 1963. L'interpretation de l'arc des Alpes occidentales. *Bull. Soc. géol. France*, **7**(5), 20–29.

Gourlay, P. and Ricou, L.E., 1983. Le jeu décrochant dextral tardif de la suture de Chamonix (Alpes françaises et suisses). *C.R. Acad. Sci. (Paris)*, **296**, 927–932.

Grosjean, G., Sue, C. and Burkhard, M., in press. Late Neogene brittle extension in the vicinity of the Simplon fault zone, central *Alps, Switzerland. Eclog. Geol. Helv.*, **96**, in press.

Herren, E., 1987. Zanskar shear zone; northeast-southwest extension within the Higher Himalayas (Ladakh, India). *Geology*, **15**, 409–413.

Hubbard, M. and Mancktelow, N.S., 1992. Lateral displacement during Neogene convergence in the western and central Alps. *Geology*, **20**, 943–946.

Kahle, H.G., Geiger, A., Buerki, B., Gubler, E., Marti, U., Wirth, B., Rothacher, M., Gurtner, W., Beutler, G., Bauersima, I. and Pfiffner, O.A., 1997. Recent crustal movements, geoid and density distribution; contribution from integrated satellite and terrestrial measurements. In: *Deep Structures of the Swiss Alps: Results of NRP20* (O.A. Pfiffner, P. Lehner, P. Heitzmann, S. Mueller and A. Steck, eds), pp. 251–259. Birkhaüser Verlag, Basel.

Kastrup, U., Zoback, M.L., Deichmann, N., Evans, K. and Giardini, D., 2004. Stress field variations in the Swiss Alps and the northern Alpine foreland derived from inversion of fault plane solutions. *J. Geophys. Res.*, **109**, B01402.

Linzer, H.G., Decker, K., Peresson, H., Mour, R.D. and Frisch, W., 2002. Balancing lateral orogenic float of the Eastern Alps. *Tectonophysics*, **354**, 211–237.

Lister, G.S. and Davis, G.A., 1989. The origin of metamorphic core complexes and detachment faults formed during Tertiary continental extension in the northern Colorado River region, USA *J. Struct. Geol.*, **11**, 65–94.

Mancel, P. and Merle, O., 1987. Kinematics of the northernpart of the Simplon line (central Alps). *Tectonophysics*, **135**, 265–275.

Mancktelow, N.S., 1985. The Simplon line: a major displacement zone in the western Lepontine Alps. *Eclog. Geol. Helv.*, **78**, 73–96.

Mancktelow, N.S., 1990. The Simplon fault zone. *Breit. Geol. Karte Schweiz (NF)*, **163**.

Mancktelow, N.S., 1992. Neogene lateral extension during convergence in the Central Alps: evidence interrelated faulting and backfolding around the Simplonpass (Switzerland). *Tectonophysics*, **215**, 295–317.

Maurer, H., Burkhard, M., Deichmann, N. and Green, G., 1997. Active tectonism in the central Alps: contrasting stress regimes north and south of the Rhone Valley. *Terra Nova*, **9**, 91–94.

Molnar, P. and Tapponnier, P., 1978. Active tectonics of Tibet. *J. Geophys. Res.*, **83**, 5361–5375.

Nievergelt, P., Liniger, M., Froitzheim, N. and Maehlmann, R.F., 1996. Early to mid Tertiary crustal extension in the Central Alps; the Turba mylonite zone (eastern Switzerland). *Tectonics*, **15**, 329–340.

Nocquet, J.-M., 2002. *Mesure de la déformation crustale en Europe occidentale par Géodésie spatiale*. Thèse de doctorat, Université de Nice.

Nocquet, J.M. and Calais, E., 2003. Crustal velocity field of western Europe from permanent GPS array solutions, 1996–2001. *Geophys. J. Int.*, **154**, 72–88.

Nocquet, J.M. and Calais, E., 2004. Geodetic measurements of crustal deformation in the Western Mediterranean and Europe. *Pure Appl. Geophys.*, **161**, 661–681.

Oldow, J.S., Ferranti, L., Lewis, D.S., Campbell, J.K., D'Argenio, B., Catalano, R., Pappone, G., Carmignani, L., Conti, P. and Aiken, C.L.V., 2002. Active fragmentation of Adria, the north African promontory, central Mediterranean orogen. *Geology*, **30**, 779–782.

Pavoni, N., 1991. Bipolarity in structure and dynamics of the Earth's mantle. *Eclog. Geol. Helv.*, **84**, 327–343.

Pavoni, N., Maurer, H.R., Roth, P. and Deichmann, N., 1997. Seismicity and seismotectonics of the Swiss Alps. In: *Deep Structures of the Swiss Alps: Results of NRP20* (O.A. Pfiffner, P. Lehner, P. Heitzmann, S. Mueller and A. Steck, eds), pp. 241–250. Birkhaüser Verlag, Basel.

Pfiffner, O.A., Ellis, S. and Beaumont, C., 2000. Collision tectonics in the Swiss Alps: insight from geodynamic modeling. *Tectonics*, **19**, 1065–1094.

Ratschbacher, L., Frisch, W., Linzer, H.-G. and Merle, O., 1991. Lateral extrusion in the Eastern Alps; part 2: structural analysis. *Tectonics*, **10**, 257–271.

Rey, P., Vanderhaeghe, O. and Teyssier, C., 2001. Gravitational collapse of the continental crust: definition, regimes and modes. *Tectonophysics*, **342**, 435–449.

Selverstone, S.M., 1988. Evidences for East–West crustal extension in the eastern Alps: implication for the unroofing history of the Tauern window. *Tectonics*, **7**, 87–105.

Seward, D. and Mancktelow, N.S., 1994. Neogene kinematics of the central and western Alps: evidence from fission-track dating. *Geology*, **22**, 803–806.

Soom, M.A., 1990. *Abkülungs und Hebungsgeschichte der Extern Massive und der Penninischen Decken beidseits des Simplon-Rhône-Linie seit dem Oligozän: Spaltspurdatierungenan Apatit/Zircon und K-Ar Datierungenan Biotit/Muscovit (Westlische Zentralalpen)*. PhD Thesis, University of Berne.

Speranza, F., Villa, I.M., Sagnotti, L., Florindo, F., Cosentino, D., Cipollari, P. and Mattei, M., 2002. Age of the Corsica–Sardinia rotation and Liguro-Provençal Basin spreading: new paleomagnetic and Ar/Ar evidence. *Tectonophysics*, **347**, 231–251.

Sperner, B., Ott, R. and Ratschbacher, L., 1993. Fault-striae analysis: a turbo pascal program package for graphical presentation and reduced stress-tensor calculation. *Computers Geosciences*, **19**, 1361–1388.

Steck, A., 1984. Structure de déformations tertiaires dans les Alpes centrales (transversale Aar–Simplon–Ossola). *Eclog. Geol. Helv.*, **77**, 55–100.

Steck, A. and Hunziker, J., 1994. The tertiary structure and thermal evolution of the central Alps – compressional and extensional structures in an orogenic belt. *Tectonophysics*, **238**, 229–254.

Sue, C., Thouvenot, F., Frechet, J. and Tricart, P., 1999. Widespread extension in the core of the western Alps revealed by earthquake analysis. *J. Geophys. Res.*, **104** (B11), 25611–25622.

Sue, C. and Tricart, P., 1999. Late Alpine brittle extension above the Frontal Pennine Thrust near Briancon, Western Alps. *Eclog. Geol. Helv.*, **92**, 171–181.

Sue, C. and Tricart, P., 2002. Widespread post-nappe normal faulting in the Internal Western Alps: a new constrain on arc dynamic. *J. Geol. Soc. (London)*, **159**, 61–70.

Sue, C. and Tricart, P., 2003. Neogene to current normal faulting in the inner western Alps: a major evolution of the late alpine tectonics. *Tectonics* **5**, 1050, doi: 1029/2002TC001426.

Tricart, P., Schwartz, S., Sue, C., Poupeau, G. and Lardeaux, J.-M., 2001. La dénudation tectonique de la zone ultradauphinoise et l'inversion du front briançonnais au sud-est du Pelvoux (Alpes Occidentales): une dynamique miocène à actuelle. *Bull. Soc. Géol. France*, **172**, 49–58.

Vigliotti, L. and Langenheim, V.E., 1995. When did Sardinia stop rotating? New paleomagnetic results. *Terra Nova*, **7**, 424–435.

Vigny, C., Chery, J., Duquesnoy, T., Jouanne, F., Ammann, J., Anzidei, M., Avouac, J.P., Barlier, F., Bayer, R., Briole, P., Calais, E., Cotton, F., Duquenne, F., Feigl, K.L., Ferhat, G., Flouzat, M., Gamond, J.F., Geiger, A., Harmel, A., Kasser, M., Laplanche, M., Le Pape, M., Martinod, J., Menard, G., Meyer, B., Ruegg, J.C., Scheubel, J.M., Scotti, O. and Vidal, G., 2002. GPS network monitors the Western Alps' deformation over a five-year period: 1993–98. *J. Geodesy*, **76**, 63–76.

Wernicke, B. and Burchfield, B.C., 1982. Modes of extensional tectonics. *J. Struct. Geol.*, **4**, 105–115.

Yamaji, A., 2000. The multiple inverse method: a new technique to separate stresses from heterogeneous fault-slip data. *J. Struct. Geol.*, **22**, 441–452.

Received 6 February 2004; revised version accepted 10 May 2004